Available online at www.sciencedirect.com
SCIENCE DIRECT®
International Journal of Mass Spectrometry 241 (2005) 1–9
International Journal of Mass Spectrometry
www.elsevier.com/locate/ijms

Wide dispersion multiple collector isotope ratio mass spectrometer

Anthony D. Appelhans*, James E. Delmore, John E. Olson

Idaho National Engineering and Environmental Laboratory, P.O. Box 1625, Idaho Falls, ID 83415, USA

Received 23 June 2004; accepted 18 October 2004
Available online 26 November 2004

Abstract

A new design for an enhanced dispersion thermal ionization multi-collector isotope ratio mass spectrometer is proposed and the results of tests with a small-scale prototype instrument are presented. The measured performance of the small-scale prototype sized for ^{6}Li and ^{7}Li is compared with the predictions of an ion optical model. The ion optical model is shown to accurately predict the measured mass dispersion, mass resolution, and general ion beam profile, providing confidence that the ion optical modeling can be applied to design of a full-scale instrument. The design concept includes a single magnetic sector and an electrostatic dispersion lens to magnify the mass dispersion so that full sized discrete dynode electron multipliers can be used to simultaneously monitor each isotope. A conceptual model is presented for a thermal ionization instrument capable of simultaneous measurement of seven isotopes in the 240 Da mass range with full size discrete dynode electron multipliers.

Keywords: Isotope ratio; Mass dispersion; Multiple collector; Magnetic sector mass spectrometer; Thermal ionization

1. Introduction

The design of thermal ionization isotope ratio mass spectrometers has been evolving to meet ever-increasing needs for higher absolute sensitivity and greater abundance sensitivity. The major development has been the addition of multiple collectors to enable simultaneous measurement of two or more isotopes [1–4]; Barnes and Hieftje provide a summary in [5]. In order to accommodate multiple collectors the mass dispersion must be increased and/or the size of the collectors reduced. In fact, most multiple collector instruments have relied on a combination of each [6]. The commonly used method for increasing the mass dispersion is special shaping of the magnet poles [2] although a double quadrupole zoom lens arrangement has also been implemented [7]. This has enabled the use of multiple miniature faraday cups combined with miniature electron multipliers arranged in an array along the focal plane of the magnetic sector. These geometries allow up to nine isotopes to be measured simultaneously, which results in improved precision of the isotope ratios. The trade off is that the abundance sensitivity is limited to $\sim 10^{6}$ at best, and is more commonly in the 10^{5} range, because of both the dark noise level of the miniature detectors, their proximity to one another [6], limited dynamic range, and physical constraints limiting filtering of stray ions and electrons.

We have taken a different approach and that is to magnify the dispersion to accommodate full sized discrete dynode electron multipliers or Faraday cups. In order to obtain the highest sensitivity, individual ion counting is required for the minor isotopes. The state of the art for full size discrete dynode multipliers is impressive, with dark counts as low as 1–2 per min. They are also very efficient, near 100% for ions of sufficient velocity [2,8]. Thus a primary design criterion is to increase the mass dispersion enough to measure up to seven isotopes simultaneously, each with a physically isolated, full size discrete dynode multiplier or Faraday cup. Since discrimination against isobaric molecular interferences is not required, the mass resolution need only be in the range of 400–800. These requirements led to a design, described herein, that relies on magnification of the mass dispersion following the mass separation sector of the mass

* Corresponding author. Tel.: +1 208 526 0862; fax: +1 208 526 8541.
E-mail address: ada2@inel.gov (A.D. Appelhans).

1387-3806/$ – see front matter © 2004 Elsevier B.V. All rights reserved.
doi:10.1016/j.ijms.2004.10.020

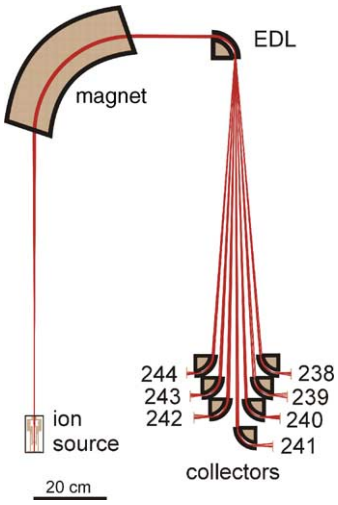

Fig. 1. Ion optics design of a wide dispersion multi-collector thermal ionization isotope ratio mass spectrometer and the calculated trajectories for ions in the mass range 238–244 Da.

spectrometer. While a similar approach has been suggested previously [9], it proposed a high voltage linear dispersion lens that produced a second focal plane. We were unable to find published reports of the proposed method put into practice. Our design does not produce a second focal plane, but rather utilizes an electrostatic dispersion lens (EDL) to magnify the dispersion between mass separated beams while decreasing the angular divergence of each beam. This increased dispersion and reduced angular divergence produced by the EDL allows the detectors to be located along the beam line where the beams are separated sufficiently to use physically isolated, full sized Faraday cups or discrete dynode multipliers for each isotope beam.

2. Conceptual model

A proposed application of the wide dispersion concept is the design of an instrument sized for simultaneous detection of heavy isotopes such as U or Pu.[1] Using Pu as an example, a SIMION [11] model of a candidate design is shown in Fig. 1, along with a set of ion trajectories. In the model, ions are produced with a thermal ionization source and are accelerated and focused using a variation of a univoltage ion lens [12]. The magnetic sector consists of a 27 cm radius magnet with non-normal entry and exit pole faces to provide stigmatic focusing, based on the magnets used in a triple sector isotope ratio mass spectrometer [13] that we have in our laboratory. The EDL physically resembles a conventional electrostatic sector analyzer (ESA); however, in this arrangement it is not operated as an energy analyzer nor does it provide any filtering (there are no entrance or exit slits), thus, we have chosen not to refer to it as an ESA but to use a name that more accurately describes its function. The EDL was sized to accommodate

[1] Patent applied for.

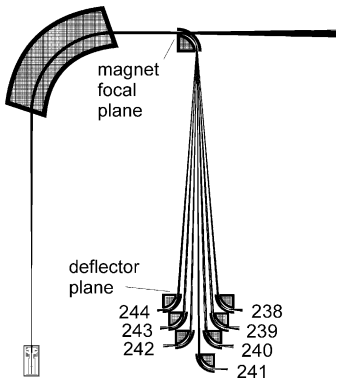

Fig. 2. Calculated ion trajectories of seven Pu isotopes with and without the EDL in place.

seven isotopes from *m/z* 238 to 244 and to disperse the beams into separate full sized pulse counting (or Faraday cup) collectors. The EDL performs two functions; it decreases the angular divergence of each beam, and magnifies the dispersion between beams. This permits the detectors to be located at a distance at which the beams are sufficiently separated to allow each beam to be diverted into a full sized, physically isolated detector. In the design of Fig. 1, each beam is diverted with a small, 90° cylindrical lens into a well-isolated detector. This geometry is anticipated to improve the abundance sensitivity, as it will discriminate against scattered ions with lower energy. This geometry also permits further energy filtering with a device such as a retarding potential lens [14] on any channel where increased abundance sensitivity is required.

Fig. 2 graphically illustrates the theoretical EDL performance. Two sets of ion trajectories are overlaid, one set with the EDL in place (identical to Fig. 1) and the second set with the EDL removed. With the EDL removed the angular divergence of the beams quickly results in the beams overlapping. Inserted, the EDL reduces the beam angular divergence and increases the separation between beams (dispersion) so that at ∼80 cm from the EDL exit the beams (∼8 mm wide) are fully isolated and separated by ∼2 cm (center to center). This spacing is sufficient for inserting the 90° deflectors without interfering with adjacent beams. Fig. 3 shows that at the magnet focal point the ratio of the beam-to-beam dispersion to

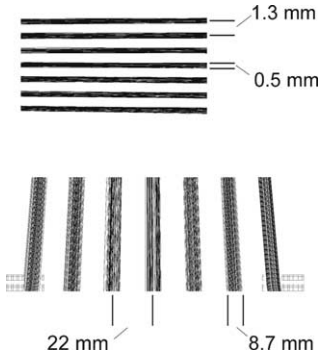

Fig. 3. Predicted beam width and separation at the magnet focal plane (top); and predicted beam width and separation at the deflector plane (bottom) for the ion trajectories shown in Fig. 2.

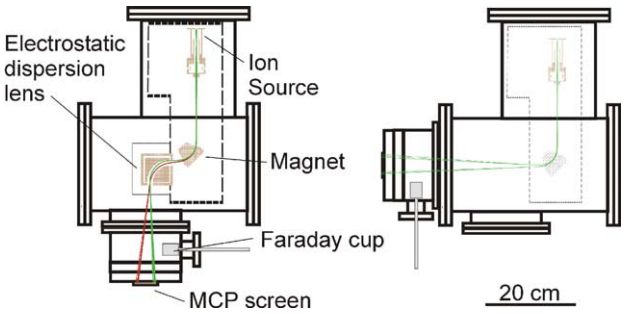

Fig. 4. Small-scale prototype wide dispersion mass spectrometer layout: configuration A (left) for beam measurements with EDL in place; and configuration B (right) for beam measurements without the EDL.

the beam width is 2.6, while at the 80 cm position after the EDL the ratio is 2.5 demonstrating that the quality of the beams has been maintained during magnification (ignoring scattering from neutral gas molecules). This theoretical performance is very encouraging; however, prior to committing to a detailed design and construction of such an instrument we have used a small-scale prototype to test the concept and verify that the ion optics model can be relied upon to predict the instrument performance. Results of experiments conducted with the small-scale instrument and a comparison with the ion optics model are presented.

3. Prototype instrument design

To verify the modeling results and demonstrate the validity of the wide dispersion concept, a prototype instrument has been designed, constructed and tested. The prototype, shown schematically in Fig. 4 and in the photograph in Fig. 5, was scaled for ^{6}Li and ^{7}Li. It included an ion gun, permanent magnet, EDL assembly, and a Faraday cup and multichannel plate image intensifier (MCP) for measuring the ion beam profiles. The ion source consisted of a Pt tube (0.7 mm i.d.) packed with a zeolite previously ion exchanged with Li. The Pt tube was spot welded to Re filament wires and heated to ~900 °C to generate the $^{6}Li^{+}$ and $^{7}Li^{+}$. The ion focusing and acceleration lens, described previously [12], produces a circular cross section ion beam whose focal point can be adjusted with an einzel lens located after the exit aperture of the acceleration stage. The typical acceleration voltage for the Li isotopes was 1600 V. The nominal one-inch radius magnet was constructed of two iron pole pieces and two permanent magnets (neodymium iron boride). The magnet gap was 6 mm, and the resulting field was ~4.15 kG, measured with a Hall probe. The pole faces of the magnet were set at 18° off normal, producing an included angle of 54°, in order to constrain beam divergence in the *Z* plane (vertical). This commonly used approach [2,13] also increases the mass dispersion as compared to normal (90°) entry and exit. The EDL consisted of two quarter-section right cylinder faced electrodes (inner radius 35 mm, outer radius 45 mm) spaced 13 mm apart and mounted in a grounded enclosure mounted on an adjustable *XY* stage (Fig. 5). The EDL was sized so that both Li isotope beams could be simultaneously viewed on the MCP, and was typically operated at ±350 V for a 1500-V beam. The ion gun and magnet were mounted on a single support plate so that they could be positioned and aligned before installation in the vacuum housing. The EDL assembly was mounted on a separate plate that was attached to the magnet support plate, linking the two assemblies within the vacuum housing (Fig. 4).

The vacuum housing, pumped with a 170 l/s turbo pump, had a base pressure of 2×10^{-7} Torr without any of the components installed. The mass spectrometer portion without the EDL pumped to this same pressure, demonstrating that the neodymium iron boride magnet did not degrade the base pressure. When the EDL was installed the base pressure increased to 2×10^{-6} Torr because the *XY* stage on which the EDL was

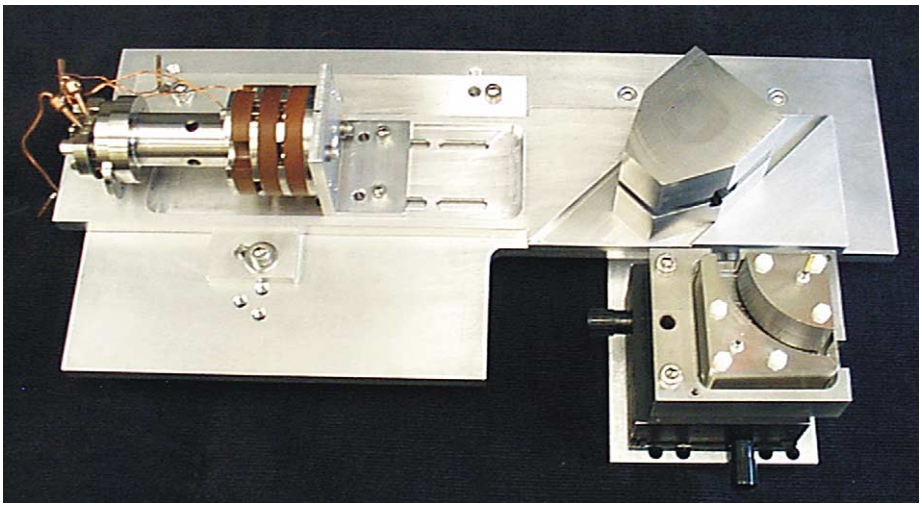

Fig. 5. Photograph of the prototype system components attached to the mounting platform. The EDL top cover has been removed in the photograph to display the electrode shape.

mounted was not designed for vacuum applications. Referring to Fig. 4, the vacuum housing was designed so that a detector assembly spool piece consisting of the Faraday cup mounted on a linear translator and the fixed-position MCP could be oriented in two positions. One of these positions allowed measurement of the ion beams after passing through the EDL, and the other with the EDL removed so that the beams came directly from the magnetic sector. The Faraday cup, mounted on a 150 mm linear translator with a resolution of 0.0254 mm, included a secondary electron suppression grid and a ground shield with a 1.3 mm × 18 mm beam aperture. In addition, a separate 152 mm extension nipple could be installed between the main vacuum housing and the detector assembly to increase the distance along the beam lines where the measurements were made. With this arrangement, measurements on the mass dispersion and the beam width could be made at two points along the beam line with and without the EDL in place.

4. Results

Experiments were conducted with the prototype instrument to measure the width of each isotope beam, the spacing between the two beams, and obtain the cross section of the beam profile with and without the EDL in place at two locations along the beam line. In addition, the ion optics model was used to predict these same measurements using the as-built dimensions and spacing of the components and the measured voltages and magnetic field from the experiments. The measured and predicted performance was then compared.

4.1. EDL in place

Initial measurements were taken with the EDL in place (configuration A of Fig. 4). The accelerating voltage of the ion source was adjusted so that both the $^{6}Li^{+}$ and $^{7}Li^{+}$ beams were visible on the MCP, and the beam current was measured with the Faraday cup as a function of lateral position. This enabled both the individual width of each beam and their relative spacing (dispersion) to be determined. The MCP was also photographed to document the shape of the beams. The Faraday cup measurements were made with an electrometer connected to a laptop computer. A simple data acquisition program was used to record the electrometer signals as a function of the Faraday cup position. Typical ion currents for $^{7}Li^{+}$ were 50–100 pA.

Fig. 6 presents the measured profile of the $^{6}Li^{+}$ and $^{7}Li^{+}$ beams. The $^{6}Li/^{7}Li$ ratio agreed reasonably well with the standard values, although no effort was made to conduct a quantitative measurement. Fig. 7 shows a photograph of the two Li beams on the MCP screen for the same conditions as Fig. 6, and the predicted beam cross section at the MCP location. The beam profiles were also measured with the extension nipple in place using all the same conditions; results are shown in Fig. 8. The ion optics model was used to predict the beam profile and spacing for these conditions. Fig. 9 presents the measured and predicted results. Note that the measured beam intensity for each beam has been normalized to 1 for ease of comparison with the model. In the simulations 20,000 ions were flown for each beam and the ions originated from random positions on the emitter at random angles. The agreement between the model predictions and the measured results demonstrates that the model can be used to predict the performance of the EDL.

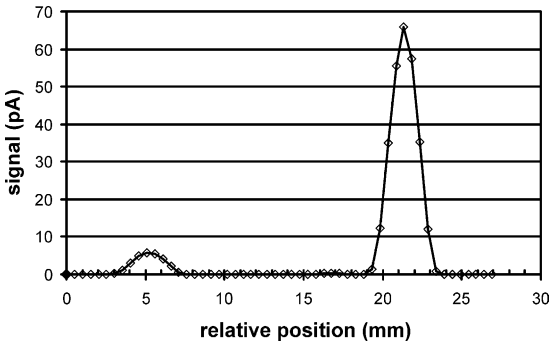

Fig. 6. Measured $^{6}Li^{+}$ and $^{7}Li^{+}$ beam profiles with the EDL in place (configuration "A" of Fig. 4).

4.2. Magnet only

Beam profiles were measured at two distances from the magnet with the EDL removed. The ion source voltages and

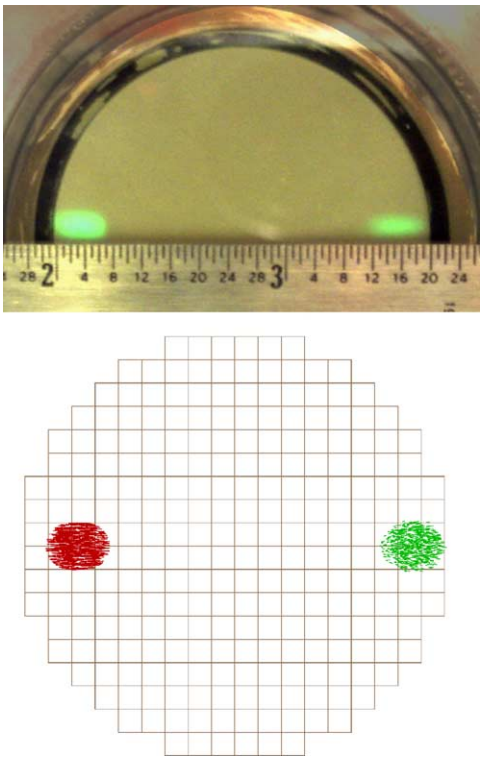

Fig. 7. $^{7}Li^{+}$ and $^{6}Li^{+}$ beam cross sections photographed on the MCP with the EDL in place (top) and as predicted with the model (bottom). (Note that the scale is in inches).

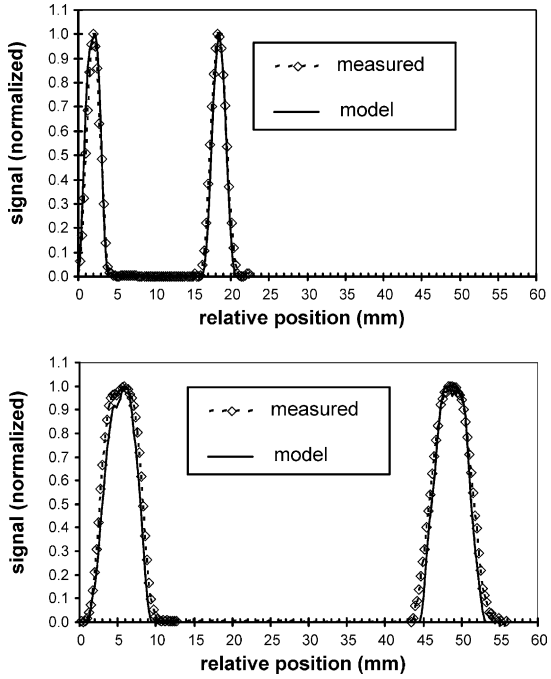

Fig. 8. $^{7}Li^{+}$ and $^{6}Li^{+}$ measured beam profiles (symbols) and the calculated profiles (solid lines), with the EDL; without (top) and with (bottom) the extension nipple. Without the extension nipple $m/\Delta m = 33.6$; with the nipple $m/\Delta m = 38.5$.

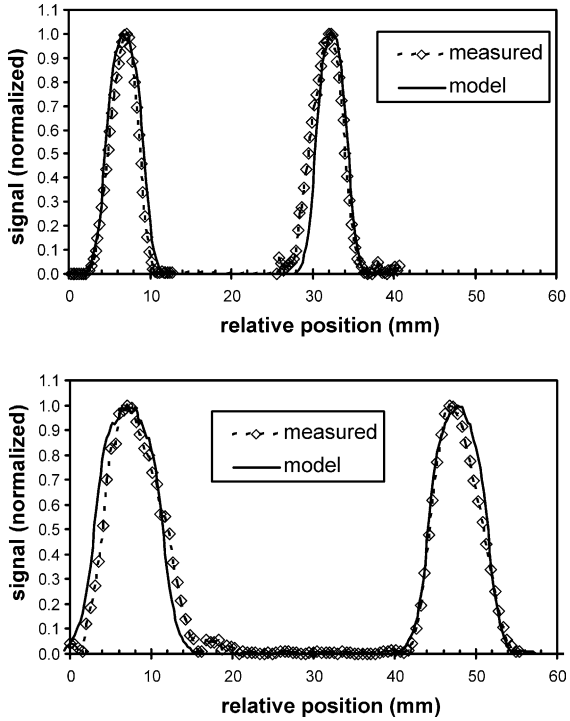

Fig. 9. $^{7}Li^{+}$ and $^{6}Li^{+}$ measured beam profiles (diamonds) and the calculated profiles (solid lines) without the EDL; without (top) and with (bottom) the extension nipple. Without the nipple $m/\Delta m = 26.6$, with the nipple $m/\Delta m = 23.1$.

magnet position were kept the same as in the previous measurements. The experimental conditions were used in the ion optics model to predict the beam profiles and mass dispersion. The profile results are shown in Fig. 10, with the beam intensities normalized to one. The calculated trajectories of the two beams along with their measured profiles at two locations are shown in Fig. 11 along with a set of ion trajectories with the EDL in place. Again the agreement between the model and the experiment was very good.

4.3. Mass dispersion

Mass dispersion is classically defined at the focal plane of the magnetic or electrostatic sector [2], typically where the detector would be located. However, for the proposed instrument design the detectors are not located at focal points, and thus the classical definition does not adequately describe the system performance. More meaningful figures of merit for the proposed design are the rate of dispersion of one beam from the other, and the angular divergence of the individual beams. By measuring the beam separation and the beam profile (width) at two points along the beam path these figures of merit can be calculated and compared. For example, using the measured beam profiles from Fig. 9 with the EDL in place, the rate of separation of the $^{6}Li^{+}$ beam from the $^{7}Li^{+}$ beam is 27 mm/152 mm (the extension nipple is 152 mm long), while for the system without the EDL in place the rate is 15 mm/152 mm. Thus there is a factor of about 2 increase in the separation rate with the EDL. At the same time that the beams are diverging one from the other, the individual beams also have an angular divergence, that is, they are expanding in width. The angular divergence of the ^{7}Li beam after the magnet (without the EDL) is 2.25°, while the angular divergence after the EDL is 1.7°. Thus with the EDL the beams are separating at about twice the rate but are increasing in width only 75% as fast as the beams without the EDL (Fig. 11 illustrates the difference). Defining the resolution, $m/\Delta m$, as the mass divided by the peak width (at 10% peak height at the measurement position), over the 152 mm interval between each measurement point the resolution increases with the EDL in place (Fig. 9) from 33.6 to 38.5 as the beams diverge, while without the EDL (Fig. 10), the resolution decreases from 26.6 to 23.1. Thus for these conditions, the EDL has doubled the rate of separation (dispersion) and provided an increased resolution (relative to the magnet-only system). Note that the EDL does not increase the resolution beyond that attained at the magnet focal point, but it does enable the resolution to be maintained as the beams disperse. This was illustrated in Fig. 3 for the conceptual model.

4.4. Beam profiles

The MCP enabled the beam cross-section profiles to be measured. The cross-section profiles illustrate the *Z* focusing of the magnet, and provide a stringent test for the ion optics model. In Figs. 12 and 13 the measured and predicted

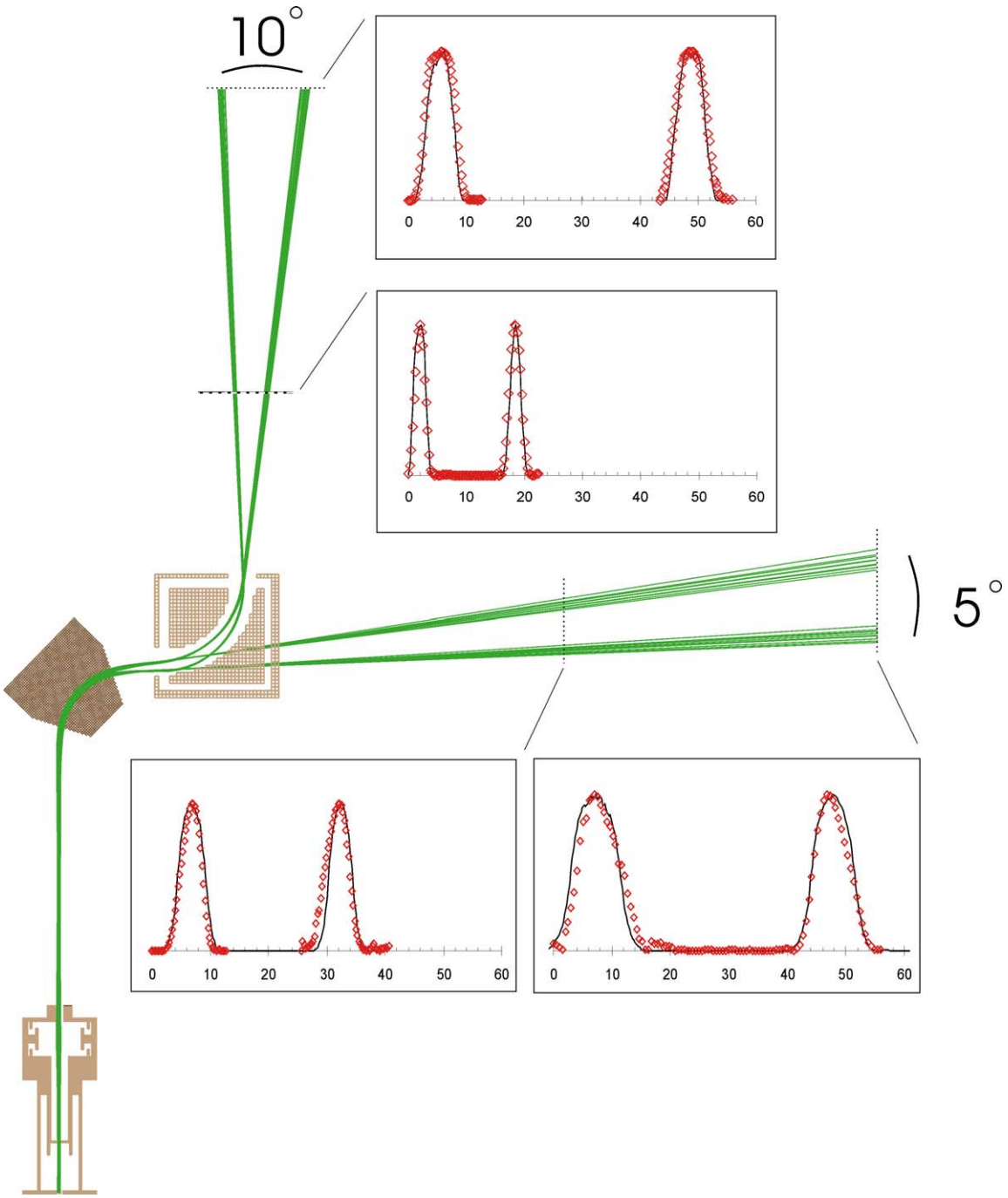

Fig. 10. Predicted ion trajectories for $^{7}Li^{+}$ and $^{6}Li^{+}$ beams, and the measured (symbols) and modeled (solid line) beam profiles at two positions along the beam line with and without the EDL in place.

cross-section profiles of the $^{7}Li^{+}$ beam at two locations along the beam line without the EDL are shown. The beam has been compressed in the *Z* (vertical) plane by the focusing action of the off-normal magnet pole faces, and the model prediction agrees very well with the measured profile. In Fig. 7 the measured and predicted profiles following the EDL were shown. In this case the beam width was predicted very well, but the measured beam height was slightly shorter than predicted. We believe this is due to slight angular misalignment between the EDL and the magnet that we are unable to accurately measure.

4.5. EDL position

The position of the EDL relative to the magnet, and thus the focal plane of the mass separated beams, affects the beam separation and the beam angular divergence. To demonstrate this a series of beam profile measurements were made with

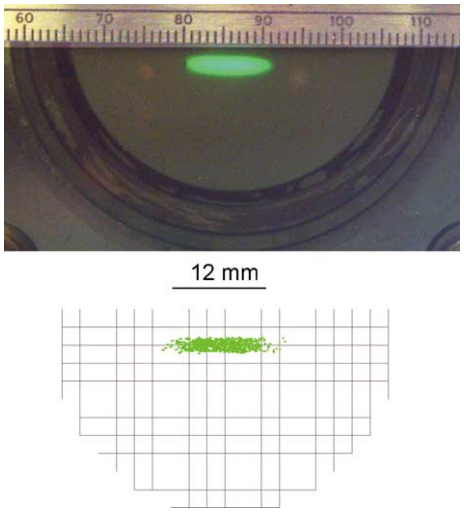

Fig. 11. Measured $^{7}Li^{+}$ beam cross section on the MCP for the short flight path without the EDL (magnet only) (top, note that scale is in mm); and predicted beam profile generated using the same voltages as in the experiment, scale is 2.3 mm/grid unit (bottom).

the EDL at three positions relative to the magnet pole face, at 16 mm, 26 mm, and 36 mm (refer to Fig. 4). All other parameters were held constant. The measured and predicted beam profiles are shown in Fig. 14, and the $^{6}Li^{+}$ peak width, dispersion and resolution for each position are listed in Table 1. The agreement between the measured and the predicted profiles is very good. The results show that relative to the spacing between the EDL and the focal plane of the magnet the resolution is essentially independent of the degree of dispersion. This implies that the dispersion can be increased by adjusting the EDL-magnet distance without compromising the resolution.

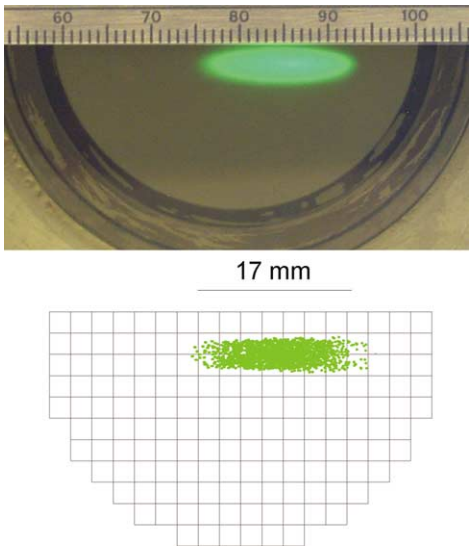

Fig. 12. $^{7}Li^{+}$ beam cross section on the MCP for the long flight path without the EDL (magnet only) (top); and, predicted beam cross section generated using the same voltages as in the experiment, scale is 2.3 mm/grid unit (bottom).

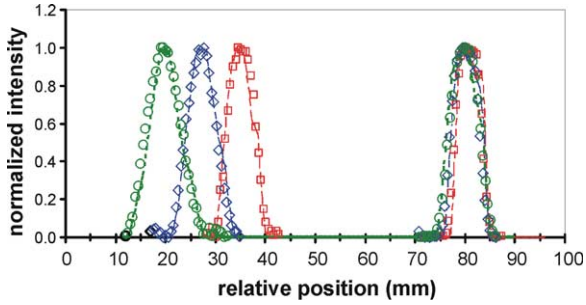

Fig. 13. Measured (symbols) and predicted (lines) beam profiles of ^{6}Li and ^{7}Li for the EDL located 16 mm (□), 26 mm (◊), and 36 mm (○) from the magnet. The $^{7}Li^{+}$ peaks have been collocated at the 80 mm position to demonstrate the change in dispersion as a function of the EDL-to-magnet distance.

Table 1
Measured and predicted peak width (mm) at 10% of the peak height, dispersion (mm), and resolution at 244 mm from the EDL exit plane for three positions of the EDL relative to the magnet pole face

Position	16 mm	26 mm	36 mm
Peak width at 10%			
Measured	9.7	11.0	13.2
Predicted	9.3	11.0	13.3
Dispersion			
Measured	45.0	52.8	60.3
Predicted	45.0	52.8	60.3
Resolution			
Measured	32.6	33.6	32.0
Predicted	34.1	33.6	31.8

All other conditions were kept constant.

Note again here that the EDL size and position for all of these experiments was not chosen to optimize the figures of merit (resolution and dispersion), but rather to demonstrate the concept and to test the ion optic model's predictive capability. What is most significant in this comparison is that the ion optics model predicts the measured behavior extremely well, and thus the model can be applied with confidence to design a larger scale instrument.

5. Discussion

The predicted performance of the prototype wide dispersion mass spectrometer agrees very well with the experimental data. Both demonstrate that by using the EDL the mass dispersion can be increased without sacrificing resolution, and indeed using the EDL the effective resolution (defined as the resolution where the beam cross section is measured, as opposed to at a focal point) increases with distance. Conventional designs dictate the detector assembly be located at the focal plane because the beam divergence is too great, and this forces the use of miniaturized detector assemblies. The EDL design reduces the beam divergence, and this characteristic makes it possible to locate detectors not at the focal plane,

where the spacing between beams is small, but rather at essentially an arbitrary distance where the beam-to-beam spacing can accommodate full sized detectors. The differences observed in the beam spacing with and without the EDL in the prototype instrument were modest; however, when this concept is applied to a larger system the effect is substantial, as illustrated in Fig. 1. For the 234 and 235 isotope trajectories shown in Fig. 1, the resolution at the magnet focal plane (without the EDL in place) is ∼700, and the beams (0.5 mm wide) are separated by 1.3 mm. With the EDL in place the resolution is ∼680 where the beams enter the individual deflection lenses, and the beams (∼9 mm wide) are separated by 22 mm (center to center). This large inter-beam spacing makes it possible to insert the 90° deflection lens into each beam line to bring the individual beams to a well-shielded collector or pulse counter. In practice, an energy filter could also be installed on each separate beam line following the 90° deflection to further improve the abundance sensitivity.

5.1. General characteristics of the EDL

Ion optical analysis with SIMION of the EDL has illustrated several characteristics important for its application. First off, it is the shape of the electric field within the EDL that controls the ion trajectories, and thus any configuration of electrodes that produces the same field shape will produce similar results. It has been observed that the maximum dispersion is obtained by using the smallest possible radius. Thus, the number of isotopes that are to be simultaneously measured and their dispersion will determine the optimum radius. The degree of magnification of dispersion between mass separated beams in the EDL is a function of the separation of the beams at the entrance to the EDL. The wider the separation at the EDL entrance, the greater the dispersion after the EDL. The criteria for placement of the EDL relative to the magnet are that point where the ratio of the beam separation to beam width is greatest and the beam angular divergence is low. Thus a magnetic sector with off-normal pole faces and the resultant lower beam divergence angles is preferred.

Because the energy spread from a thermal ionization source is small (∼0.1 eV), no slits are necessary in this design to obtain the required mass dispersion and resolution. A slit-less system also has very high ion transmission efficiency and reduces the number of scattered ions that can degrade the abundance sensitivity. It is anticipated that coupling the wide dispersion multiple collector design with the total evaporation method [15] will enable measurement of wide isotope ratios from extremely small samples with very high sensitivity.

5.2. Limitations

The design proposed herein, as most others, inherently involves trade offs between different aspects of a measurement. In this case the ability to control the mass resolution with slits has been deferred and will undoubtedly make some practitioners uncomfortable. And indeed the lack of slits, and the concomitant modest resolution, place demands on both the energy spread of the ion source and the isobaric purity of the sample. The model predicts that the energy spread typical of conventional thermal ionization sources is acceptable. However, for the EDL concept to be used with ion sources that produce a wider energy spread, an energy filter such as an electrostatic energy analyzer (E) would need to be inserted in the beam line prior to the magnetic sector (B). Thus a conventional EB configuration with an energy-resolving slit in the E sector but without a mass resolving slit in the B sector could provide mass resolved beams with sufficiently low energy spread for the EDL concept to be applied, albeit with a loss of sensitivity due to the ions discarded in the E sector.

In both the small-scale prototype instrument and in the model of the full sized instrument, the magnet is equipped with off-normal pole faces in order to provide focusing in the *Z* plane. If a magnet with normal pole faces was used, the beam would expand in the *Z* plane and the losses would be significant since the flight path after the EDL is long. Thus efficient application of the EDL concept requires the *Z* focusing strength of the magnet be matched with the length of the flight path to the detectors.

6. Conclusions

A new design for a thermal ionization multi-collector isotope ratio mass spectrometer that utilizes an electrostatic dispersion lens to magnify the mass dispersion while constraining beam divergence has been proposed and the results of tests of a small-scale prototype instrument were presented. The measured performance of the small-scale prototype sized for ^{6}Li and ^{7}Li compared with the predictions of an ion optical model showed that the ion optical model accurately predicted the measured mass dispersion, mass resolution, and general ion beam profile, providing confidence that the ion optical modeling can be applied to design of a full-scale instrument. A conceptual model was presented for an instrument capable of simultaneous measurement of seven isotopes in the 238–244 Da mass range in which each isotope can be measured with an isolated, full sized, discrete dynode electron multiplier. It is anticipated that coupling the wide dispersion multiple collector design with the total evaporation method will enable measurement of wide isotope ratios from extremely small samples with very high sensitivity.

The B/EDL configuration used in the current instrument should be appropriate for any ion source with a narrow energy spread. The design could also be adapted for an ion source with a broad energy spread if an electrostatic sector was included to control the ion energy spread (for example an E/B/EDL configuration).

Acknowledgements

The authors thank M.J. Ward for assistance in mechanical design and fabrication of components of the prototype

instrument. This research was supported by the United States Department of Energy under contract DE-AC-07-99ID13727 BBWI.

References

[1] S. Richter, A. Alonso, W. De Bolle, R. Wellum, P.D.P. Taylor, Int. J. Mass Spectrom. 193 (1999) 9.
[2] I.T. Platzner, Modern Isotope Ratio Mass Spectrometry, Wiley, New York, 1997.
[3] S. Richter, S.A. Goldberg, Int. J. Mass Spectrom. 229 (2003) 181.
[4] Yokoyama Tetsuya, Makishima Akio, Nakamura Eizo, Chem. Geol. 181 (2001) 1.
[5] J.H. Barnes IV, G.M. Hieftje, Int. J. Mass Spectrom. 238 (2004) 33.
[6] www.nu-ins.com/npdetail.html; http://www.gvinstruments.co.uk/isoprobeT1.htm; www.thermo.com.
[7] N.S. Belshaw, P.A. Freedman, R.K. O'Nions, M. Frank, Y. Guo, Int. J. Mass Spectrom. 181 (1998) 51.
[8] S. Richter, S.A. Goldberg, P.B. Mason, A.J. Traina, J.B. Schwieters, Int. J. Mass Spectrom. 206 (2001) 105.
[9] Brown, Carlson, Shirey, U.S. Patent 5,220,167.
[11] D.A. Dahl, Int. J. Mass Spectrom. 200 (2000) 3.
[12] D.A. Dahl, A.D. Appelhans, M.B. Ward, Int. J. Mass Spectrom. Ion Process. 189 (1999) 47.
[13] J.J. Stoffel(s), H.J. Laue, Int. J. Mass Spectrom. Ion Process. 105 (1991) 225.
[14] P. van Calsteren, J.B. Schwieters, Int. J. Mass Spectrom. Ion Process. 146/147 (1995) 119.
[15] R. Fiedler, Int. J. Mass Spectrom. Ion Process. 146/147 (1995) 91.